International Journal of Control, Automation and Systems 15(6) (2017) 2906-2920
http://dx.doi.org/10.1007/s12555-016-0569-6
ISSN:1598-6446 eISSN:2005-4092
http://www.springer.com/12555

Adaptive Fuzzy Sliding Control Enhanced by Compensation for Explicitly Unidentified Aspects

Sy Dzung Nguyen, Seung-Bok Choi, and Tae-Il Seo*

Abstract: Reality shows that 1) the effectiveness of compensators for uncertainty and disturbance (UAD) depends deeply on UAD's time varying rate (TVR), and 2) controlling a system over a network introduces different constraints and conditions, in which some of these are variable delays in control signal, packet losses, data quantization, safety, and security. This paper presents a new design of fuzzy sliding mode control (FSMC) enhanced by compensation for UAD using a disturbance observer (DO), named DO-FSMC, for a class of nonlinear systems subjected to UAD. First, in order to weaken partly the negative influence of TVR of UAD on the compensation effectiveness, we separate explicitly unidentified aspects into two groups, one related to the model error while the other coming from external disturbances, to distinctly consider. To stamp out the chattering status and reduce calculating cost, we propose an adaptive gain updated directly based on the sliding surface convergence status, to which two new control laws, one for the FSMC and the other for the DO-FSMC, are given via Lyapunov stability analysis. In order to evaluate the DO-FSMC, simulations as well as surveys based on a real semi-active suspension system using a Magnetorheological damper (MRD) with measured datasets are performed. The results obtained from the surveys coincide with the theoretical analysis which show that the competence to stamp out vibration is the advantage of the proposed method compared with the other published methods.

Keywords: Disturbance observer, fuzzy sliding control, nonlinear system, uncertainty and disturbance estimator.

1. INTRODUCTION

Generally, control systems always operate in disturbance and uncertainty conditions coming from the mathematical model errors and external disturbances. Impacting of explicitly unidentified aspects as well as the nonlinear attributes of the controlled plants on the systems are always challenges facing the design of controllers. Many solutions can be used to overcome partly this issue such as fuzzy logic (FL) [1,2], sliding mode control (SMC) [3–6], estimating UAD by different ways to establish compensate parameters [7], or combination models [8–11].

Regarding FL, there have been significant research efforts to practically contribute to the fuzzy theory as well as its applications [12–17]. This is an innovation approach to build solutions for multi-parameter and nonlinear problems as well as lack of information or using inexplicit information to describe systems [15]. By using FL, the relationship between the input and output space can be established more simply with higher accuracy rate than that based on conventional techniques [18–20]. Generally, for FL, the ability to infer via human experience and/or experimental results is used to illustrate systems. Related to control, this ability of FL is exploited to express the controlled plants as well as to depict control strategies. By this way, fuzzy controllers can handle the complex, nonlinear and inexplicit relations to depict and control systems in the presence of UAD. With essential advantages and basic features as above mentioned, fuzzy logic has been applied successfully in many different fields in which controlling nonlinear engineering systems is one of typical instances [21–23]. Related to this work, it can observe that adaptive fuzzy control and, especially, fuzzy sliding mode control (FSMC) are prevalent options [21, 22]. FSMC can bring into playing the advantages of both, FL as well as SMC.

Advantages of SMC are simplicity of implementation, robustness against plant's uncertainty and external disturbance, insensitivity to external effects, and easy to coordinate with other mathematical tools [4,24–26]. SMC is a nonlinear control method with a variable structure. By

Manuscript received September 12, 2016; revised March 2, 2017; accepted March 27, 2017. Recommended by Associate Editor Sung Jin Yoo under the direction of Editor Euntai Kim. This research was supported by the Post-doctor Research Program (2016) through the Incheon National University (INU), Incheon, Korea.

Sy Dzung Nguyen is with Division of Computational Mechatronics, Institute for Computational Science, Ton Duc Thang University, Ho Chi Minh City, Vietnam; Faculty of Electrical and Electronics Engineering, Ton Duc Thang University, Ho Chi Minh City, Vietnam (e-mail: nguyensydung@tdt.edu.vn). Seung-Bok Choi is with Department of Mechanical Engineering, Smart Structures and Systems Laboratory, Inha University, Korea (e-mail: seungbok@inha.ac.kr). Tae-Il Seo is with Department of Mechanical Engineering, Incheon National University, Korea (e-mail: tiseo@inu.ac.kr).
* Corresponding author.

application of a discontinuous control signal to force the system to slide along a cross-section of the system's normal behavior, the sliding mode controller can alter the dynamics of a nonlinear system [27,28]. Firstly, a switching surface in the state space called the sliding surface is chosen to reflect the given control aim. A process consisting of two phases, approaching and maintaining, is then carried out. The system is controlled to direct towards the sliding surface in the first phase and then uphold switching along the surface during the second phase. If the dynamic process is stable, the states of the system are almost always kept on this switching surface. The ability to reach the sliding surface and keep system states in it without chattering phenomenon expresses the quality of the controller. These targets of SMC can be met better via the combination with FL in the well-known structure named FSMC. As a type of the nonlinear dynamic inversion control models with the basic strong points, FSMC has been widely employed in many fields [3,9,10,29]. In case that the impact of UAD on the system needs to be estimated, the design of the FSMC and compensator for UAD can be independently carried out [30,31].

For building compensators for explicitly unidentified aspects, reality has been shown that the effectiveness of this work deeply depends on TVR of UAD. In [30], a controller for a MRD suspension system of train cars was established. In this, the authors proved that when TVR of UAD increased, the quality of the controller was reduced. For the chattering problem of SMC, many solutions have been given. In [32], Mohammad *et al.* presented an optimal adaptive fuzzy sliding mode controller for a class of nonlinear systems subjected to UAD. An adaptive fuzzy structure was applied to approximate maximum boundary of uncertainty aspects. A fuzzy gain was established to prevent the system from the chattering status. In the controller, however, a difficulty can be seen related to using the feedback linearization approach which exists latent uncertainty attributes. Besides, the high calculating cost coming from the fuzzy gain is also an issue of large network systems. This is much the same as the defect of the method presented in [33], where a fuzzy structure was built to stamp out the chattering. FL systems own advantages as above mentioned, these, however, result in increasing the calculating cost in many applications. Khanesar *et al.* [34] showed that controlling a system over a network introduces different constraints and conditions. Some of these constraints and conditions are variable delays in control signal, packet losses, data quantization, safety, and security.

Consequently, in this paper, we present a new controller for a class of nonlinear systems subjected to UAD. The controller named DO-FSMC is constituted of a fuzzy sliding mode controller (FSMC) enhanced by a compensator for UAD based on a disturbance observer (DO). In the approach, explicitly unidentified aspects are separated into two groups to distinctly consider. The reason for this is to weaken partly the negative influence of TVR of UAD on the compensation effectiveness. The first group related to model errors is estimated indirectly via the FSMC. The other group consisting of external disturbances is compensated via the compensator. In order to deal with the chattering issue as well as the calculating cost, we propose an adaptive gain, which is updated directly via the time varying status of the sliding surface. Based on Lyapunov stability analysis and the proposed adaptive gain, two new control laws for the nonlinear systems subjected to uncertainty with or without disturbance are presented. In order to evaluate the method, simulations as well as surveys based on a real semi-active MRD suspension system are performed.

There are four main contributions of the paper deployed via a control strategy proposed in Section 2. The first one is a new adaptive control law for a class of SISO n-*th* order nonlinear systems subjected to uncertainty without disturbance which is depicted by the FSMC. The second one is the DO-based compensator for external disturbance. The third one relates to a new adaptive control law for a class of SISO n-*th* order nonlinear systems in the presence of UAD which is presented via the DO-FSMC. Related to these works, analyzing the convergence ability of the DO as well as the stability attributes of the FSMC and DO-FSMC are expressed in Theorems 1-3. Finally, real surveys via an experimental apparatus are seen as the fourth contribution.

The paper is organized as follows: After the instruction section, the issue formulations and the corresponding solutions are mentioned in Section 2, which relate to the DO, FSMC and DO-FSMC. In Section 3, the design of the FSMC is presented while building the DO and establishing the DO-FSMC are carried out in Section 4. Surveys for evaluating the proposed method are shown in Section 5, to which the relative conclusions are stated in the Section 6.

2. ISSUE FORMULATION AND SOLUTIONS

Consider a general class of SISO n-*th* order nonlinear systems subjected to UAD expressed as follows:

$$\begin{cases} x^{(n)} = f_0(x,\dot{x},...,x^{(n-1)},t) \\ \qquad + g_{01}(x,\dot{x},...,x^{(n-1)},t)u(t) + g_{02}(t)D(t), \\ y = x, \end{cases} \quad (1)$$

in which $f_0(.)$, $g_{01}(.)$, $g_{02}(.)$ are known functions, assuming $g_{02}(.) > 0$; $D(t)$ is the unknown time-dependent parameter expressing explicitly unidentified aspects which consist of both, uncertainties from the mathematical model errors and external disturbances; $u(t)$ is control signal; $y(t)$ is the output. Let $\mathbf{x} = [x_1, x_2, ..., x_n]^T =$

$[x,\dot{x},...,x^{(n-1)}]^T \in R^n$ be the state variable vector depicting the system that is supposed to be observable. The aim here is to determine the control law $u(t)$ such that the state$\mathbf{x} = \mathbf{x}(t)$tracks the desired reference state $\mathbf{x}_d(t)$ in the presence of $D(t)$.

There are two issues to be considered in this study. The first one is to reduce the calculating cost in order to reduce the time delay of the control system. The second one is to find out a reasonable approach to specify the control law $u(t)$ in the presence of UAD (or $D(t)$). Reality shows that the effectiveness of compensators for $D(t)$ is reduced if its TVR increases [30].

For the first issue, the idea of seeking a solution for improving the calculating cost derives from [32–34]. In [32, 33], FSMCs with fuzzy gains ρ were applied. They are essential options to well stamp out the chattering phenomenon, however, the calculating time increases, which results in increasing time delay [34]. Hence, we propose an adaptive gain ρ_{ad}, which can be calculated directly and updated adaptively based on the convergent status of the sliding surface. This will be detailed in Theorem 1.

Regarding to the second issue, in order to weaken partly the negative influence of TVR of UAD on the effectiveness of compensation for UAD, explicitly unidentified aspects are partitioned to distinctly consider. Namely, $D(t)$ is separated into two groups corresponding to external disturbances, denoted by $d(t)$, and uncertainty related to the model error to deal individually. Thus, together with taking note of the state variable vector defined above, (1) can be re-expressed as:

$$\begin{cases} \dot{x}_1 = x_2, \\ \quad \vdots \\ \dot{x}_{n-1} = x_n, \\ \dot{x}_n = x^{(n)} = f(\mathbf{x},t) + g_1(\mathbf{x},t)\,u(t) + g_2(t)d(t), \\ y = x_1. \end{cases} \tag{2}$$

It is assumed that the TVR of $d(t)$ is slow enough and the upper bound exists, $|d(t)| \le d_0$. In (1), the unknown model error exists in $D(t)$, while in (2), it has been individually observed by $f(.)$ and $g_1(.)$ themselves, hence $f(.)$ and $g_1(.)$ become unknown nonlinear functions needing to be identified. Thus, instead of building the control law including the observer of $D(t)$ in (1), we build another control law via estimating $\hat{d}(t)$ of $d(t)$ only as well as $\hat{f}(.)$ and $\hat{g}_1(.)$ of $f(.)$ and $g_1(.)$ in (2). By this way, the negative influence of TVR of UAD on the effectiveness of compensation for UAD can be weakened, since, in general, the TVR of $d(t)$ only is lower than that of $D(t)$, as well as $d_0 \le D_0$.

For this aim, we propose the controller DO-FSMC constituted of the FSMC and DO to set up the control signal $u(t)$ as below:

$$u(t) = u_s(t) + u_c(t), \tag{3}$$

where $u_s(t)$ is calculated by the FSMC while $u_c(t)$ is specified by the DO-based compensator.

Remark 1: The solution of the DO-FSMC for dealing with UDA is as follows. Disturbance $d(t)$ is compensated by the DO-based compensator while uncertainty due to the model errors is compensated by the ability to infer of the fuzzy logic system taking part in the FSMC. This content will be detailed in Subsection 3.2 related to the approximation of the unknown functions $f(.)$ and $g_1(.)$ in (2).

Remark 2: The design of the FSMC and DO is carried as follows. For the FSMC, it is relied on (2) without disturbance, while for the DO, it is investigated via the known functions $f_0(.)$, $g_{01}(.)$ and $g_{02}(.)$ of (1). By this way, the convergence ability of the DO as well as the stability attributes of the FSMC and DO-FSMC will be proved in Theorems 1-3.

3. DESIGNING THE FSMC

The proposed FSMC is built based on system (2) without disturbance. The FSMC is employed for a class of SISO n-th order nonlinear systems subjected to uncertainty without disturbance.

3.1. A framework based on SMC

Let $\mathbf{e}(t)$ is the error vector expressing the difference between the state vector and the corresponding desired state vector

$$\mathbf{e}(t) = \mathbf{x}(t) - \mathbf{x}_d(t) = [e,\dot{e},...,e^{(n-1)}]^T \in R^n. \tag{4}$$

A sliding surface $S(\mathbf{x})$ is then defined via the error vector as follows

$$S(\mathbf{x}) = a_1 e + a_2 \dot{e} + ,...,+ a_{n-1} e^{(n-2)} + e^{(n-1)} = \mathbf{a}^T \mathbf{e}(t), \tag{5}$$

where $\mathbf{a} = [a_1,...,a_{n-1}]^T$is vector of Hurwitizian polynomial $H = s^{n-1} + a_{n-1}s^{n-2} + ... + a_1$, which has all poles to be located in the left half of the complex co-ordinate plane,$s$is the Laplace operator. Based on $S(\mathbf{x}(t))$ and assume that $\mathbf{e}(0) = 0$, the control issue here can be seen as determining the control law $u(t)$ to which $S(\mathbf{x}(t)) \to 0$ and then, $\mathbf{e}(t)$ is remained on the sliding surface during system's operating process. To do this, the following process is performed.

Based on the state vector, a Lyapunov candidate function is chosen as in (6),

$$V_0(\mathbf{x}) = \frac{1}{2} S(\mathbf{x})^2. \tag{6}$$

The time derivation of this function is then given as (7),

$$\frac{d}{dt} V_0(\mathbf{x}) = S(\mathbf{x}) \frac{d}{dt} S(\mathbf{x}) = S(\mathbf{x}) \dot{S}(\mathbf{x}). \tag{7}$$

Be noted here that $V_0(0) = 0$ and $V_0(\mathbf{x}) \ge 0$; $\forall x(t) | t > 0$. Hence from (7), we can infer that if the control law $u(t)$ is

used so that

$$\dot{S}(\mathbf{x}) = -\rho \operatorname{sgn}(S(\mathbf{x})), \tag{8}$$

where ρ is a positive coefficient, then $S(\mathbf{x}) \to 0$ is a stable Lyaponov process. As mentioned in Section 2, in the process of calculating $u_s(t)$, disturbance $d(t)$ is overlooked. From (8), (5), (4) and (2), the feedback control signal such that $\mathbf{e}(t) \to 0$ (or $\mathbf{x} \to \mathbf{x}_d$) when $t \to \infty$ can be inferred as below:

$$u_s(t) = \frac{1}{g_1(\mathbf{x},t)}\left(-\sum_{i=1}^{n-1} a_i e^{(i)} - f(\mathbf{x},t) + x_d^{(n)} - h(\mathbf{x},t)\right), \tag{9}$$

where

$$h(\mathbf{x},t) = \rho \operatorname{sgn}(S(\mathbf{x})). \tag{10}$$

To calculate $u_s(t)$ in (9), functions $g_1(\mathbf{x},t)$, $f(\mathbf{x},t)$ and $h(\mathbf{x},t)$ need to be determined.

For $g_1(\mathbf{x},t)$ and $f(\mathbf{x},t)$, we establish approximation functions $\hat{g}_1(\mathbf{x},t)$ and $\hat{f}(\mathbf{x},t)$ via fuzzy logic, which will be presented in the next subsection. Related to $h(\mathbf{x},t)$, there have been some different ways. In [3], [32] and [33], in order to avoid the chattering phenomenon, fuzzy gains were used. In [21], a PI control action was established to keep the states in a limited boundary layer. It can observe that increasing the calculating cost related to these fuzzy structures is the common difficulty of these solutions. Khanesar *et al.* [34] showed that controlling a system over a network introduces different constraints and conditions, to which, some variable delays in control signal, packet losses, data quantization may appear. To overcome these issues, we propose $h(\mathbf{x},t)$ as in (11) with an adaptive gain ρ_{ad} as in (12) together with using a boundary layer neighboring the sliding surface as in (13). It is updated directly based on value of the sliding surface, which will be detailed in Theorem 1.

$$h(\mathbf{x},t) = \rho_{ad} \operatorname{sat}\left(S(\mathbf{x})/\Phi\right), \tag{11}$$

$$\rho_{ad} = k_1(t)\left(1 - \exp\left(-k_2 |S(\mathbf{x})|\right)\right), \tag{12}$$

where k_2 is an adaptive positive coefficient chosen by the designer while $k_1 = k_1(t)$ is an adaptive coefficient whose update law is based on the sliding surface convergence status. In (11), in order to avoid the chattering phenomenon, as usual, function sgn(.) as in (10) was replaced with function sat(.). Here, we used the function defined as in [9]:

$$\operatorname{sat}\left(S/\Phi\right) = \begin{cases} \operatorname{sgn}\left(S/\Phi\right) & \text{if} \quad \left|S/\Phi\right| > 1, \\ S/\Phi \quad \text{if} \quad \left|S/\Phi\right| \le 1, \end{cases} \tag{13}$$

where Φ is the boundary layer neighboring the sliding surface to which $|S(\mathbf{x},t)| \le \Phi \ \forall(\mathbf{x},t)$. This keeps the sliding surface value in an interval range.

Remark 3: Consider the features of parameter ρ_{ad} ($0 \le \rho_{ad} \le k_1(t)$) in (12). If $|S(\mathbf{x})| \to 0$ then $\rho_{ad} \to 0$ (and $h(\mathbf{x},t) \to 0$). The aim of this solution is to make the control signal $u_s(t)$ in (9) vary as slowly as possible to uphold the system present states corresponding to $|S(\mathbf{x})| << 1$ (meaning $|\mathbf{e}(t)| = |\mathbf{x}(t) - \mathbf{x}_d(t)|$ to be small). The effectiveness of this tendency is enhanced by combining with the role of $k_1(t)$ which is updated as in (25) to guarantee stability of the system. This aspect will be presented in Theorem 1. Inversely, if $|S(\mathbf{x})|$ increases thenρ_{ad}increases exponentially. In case that $|S(\mathbf{x})| \to +\infty$, then $\rho_{ad} \to k_1$. This feature is really significant. When $|S(\mathbf{x})|$ becomes smaller, ρ_{ad} adjusts itself to a smaller value. Thereby, the control signal can rapidly reaches to a smaller value, which positively reduces the chattering phenomenon to protect the system. Inversely, if $|S(\mathbf{x})|$ becomes greater, $\rho_{ad}$and then the control signal will increase rapidly to prevent the unstable status.

3.2. Fuzzy solution for the SMC

In (9), functions $g_1(\mathbf{x},t)$, $f(\mathbf{x},t)$ and time parameter $k_1(t)$ of $h(\mathbf{x},t)$ from the SMC need to be specified. For the functions we use a fuzzy solution for their approximations $\hat{g}_1(\mathbf{x},t)$, $\hat{f}(\mathbf{x},t)$. Related to $k_1(t)$, an adaptive solution is proposed. As a result, we obtain (14):

$$u_s(t) = \frac{1}{\hat{g}_1(\mathbf{x},t)}\left(-\sum_{i=1}^{n-1} a_i e^{(i)} - \hat{f}(\mathbf{x},t) + x_d^{(n)} - h(\mathbf{x},t)\right), \tag{14}$$

These contents are shown as below:

3.2.1 Fuzzy solution

The fuzzy solution presented Ho *et al.* [21] is used to create an initial frame, to which the FSMC will be accomplished. By this, $\hat{g}_1(\mathbf{x},t)$ and $\hat{f}(\mathbf{x},t)$ in (14) can be approximated via fuzzy systems MISO, n input variables and m fuzzy laws. The i-th fuzzy law is written as below:

$$\begin{aligned} R^{(i)}: \quad & \text{IF } x_1 \text{ is } A_1^i, \text{ AND}, ..., \text{AND } x_n \text{ is } A_n^i \\ & \text{THEN } y \text{ is } B^i \quad (i = 1...m), \end{aligned}$$

where A_j^i, $j = 1, ..., n$, is the fuzzy set in the input space related to the physical parameter x_j and the i-th fuzzy law while $B^i$is the corresponding fuzzy set in the output space.

By using the center-average defuzzification, the output is calculated by

$$y(\mathbf{x}) = \left(\sum_{i=1}^{m} y^i \mu_{A^i}(\mathbf{x})\right) \Big/ \sum_{i=1}^{m} \mu_{A^i}(\mathbf{x}). \tag{15}$$

In (15), $\mu_{A^i}(\mathbf{x})$ is value of the membership function in the input fuzzy space of $\mathbf{x}(t)$. If the product law is used, $A^i = A_1^i \times ... \times A_n^i$, then $\mu_{A^i}(\mathbf{x}) = \prod_{j=1}^{n} \mu_{A_j^i}(x_j)$. Thus, (15) becomes:

$$y(\mathbf{x}) = \left(\sum_{i=1}^{m} y^i \prod_{j=1}^{n} \mu_{A_j^i}(x_j)\right) \Big/ \sum_{i=1}^{m} \prod_{j=1}^{n} \mu_{A_j^i}(x_j). \tag{16}$$

Value y^i, $i = 1, ..., m$, can be determined by the well-known methods via the fuzzy set in the output space. For simplicity, in this paper it is calculated via the singleton fuzzification. For short, (16) is re-expressed as follows:

$$y(\mathbf{x}) = \boldsymbol{\varphi}^T \boldsymbol{\lambda}(\mathbf{x}) \tag{17}$$

in which,

$$\boldsymbol{\varphi} = [y^1, ..., y^m]^T;\ \boldsymbol{\lambda}(\mathbf{x}) = \left[\lambda^1(\mathbf{x}), ..., \lambda^m(\mathbf{x})\right]^T, \tag{18}$$

$$\lambda^i(\mathbf{x}) = \left(\prod_{j=1}^{n} \mu_{A_j^i}(x_j)\right) \Big/ \sum_{i=1}^{m}\prod_{j=1}^{n} \mu_{A_j^i}(x_j). \tag{19}$$

3.2.2 Control law of the FSMC

Theorem 1: Control system (2) without disturbance is controlled by control law (14), in which,

$$h(\mathbf{x},t) = k_1(t)\left(1 - \exp(-k_2\left|S(\mathbf{x})\right|)\right) \operatorname{sat}\left(S(\mathbf{x})/\Phi\right); \tag{20}$$

$\hat{g}_1(\mathbf{x},\boldsymbol{\varphi}_g) = \boldsymbol{\varphi}_g^T\boldsymbol{\lambda}(\mathbf{x})$ and $\hat{f}(\mathbf{x},\boldsymbol{\varphi}_f) = \boldsymbol{\varphi}_f^T\boldsymbol{\lambda}(\mathbf{x})$ are fuzzy approximate functions as in (17); $\boldsymbol{\lambda}(\mathbf{x})$, $\boldsymbol{\varphi}_f$ and $\boldsymbol{\varphi}_g$ are vectors given in (18); $k_1 = k_1(t)$ is an adaptive coefficient; k_2 is a positive coefficient chosen by designer; Φ is the required boundary layer of the sliding surface to which $|S(\mathbf{x},t)| \le \Phi\ \forall(\mathbf{x},t)$. Let $\boldsymbol{\varphi}_f^*$ and $\boldsymbol{\varphi}_g^*$ be the optimal vectors of $\boldsymbol{\varphi}_f$ and $\boldsymbol{\varphi}_g$ as below:

$$\boldsymbol{\varphi}_f^* = \arg\min_{\boldsymbol{\varphi}_f \subset \Im_f}\left(\sup\left|\hat{f}(\mathbf{x},\boldsymbol{\varphi}_f^*) - f(\mathbf{x},t)\right|\right), \tag{21}$$

$$\boldsymbol{\varphi}_g^* = \arg\min_{\boldsymbol{\varphi}_g \subset \Im_g}\left(\sup\left|\hat{g}_1(\mathbf{x},\boldsymbol{\varphi}_g^*) - g_1(\mathbf{x},t)\right|\right), \tag{22}$$

where $\Im_f = \{\boldsymbol{\varphi}_f \,|\, \|\boldsymbol{\varphi}_f\| \le M_f\}$, $\Im_g = \{\boldsymbol{\varphi}_g \,|\, \|\boldsymbol{\varphi}_g\| \le M_g\}$; M_f and M_g are design parameters. Let $\Omega(\mathbf{x},\boldsymbol{\varphi}_f,\boldsymbol{\varphi}_g)$ be a function defined as in (23):

$$\begin{aligned}\Omega(\mathbf{x},\boldsymbol{\varphi}_f,\boldsymbol{\varphi}_g) =& f(\mathbf{x},t) - \hat{f}(\mathbf{x},\boldsymbol{\varphi}_f^*)\\ &+ \left(g_1(\mathbf{x},t) - \hat{g}_1(\mathbf{x},\boldsymbol{\varphi}_g^*)\right)u_s(t).\end{aligned} \tag{23}$$

Assume that Ω is a bounded function, $|\Omega(\mathbf{x},\boldsymbol{\varphi}_f,\boldsymbol{\varphi}_g)| \le \Omega_0$. Then, $\mathbf{e}(t) \to 0$ (4) or $\mathbf{x} \to \mathbf{x}_d$ when $t \to \infty$ is a stable Lyaponov process if the following update laws are adopted:

$$\dot{\boldsymbol{\varphi}}_f = S(\mathbf{x})\boldsymbol{\lambda}(\mathbf{x});\ \dot{\boldsymbol{\varphi}}_g = S(\mathbf{x})\boldsymbol{\lambda}(\mathbf{x})u_s(t); \tag{24}$$

$$k_1(t) = \begin{cases} \xi\dfrac{\Omega_0\Phi}{(|S(\mathbf{x})|+\varepsilon)(1+\varepsilon-\exp(-k_2|S(\mathbf{x})|))} & \text{if } |S(\mathbf{x})| \le \Phi,\\ \xi\dfrac{\Omega_0}{1-\exp(-k_2|S(\mathbf{x})|)+\varepsilon} & \text{if } |S(\mathbf{x})| > \Phi, \end{cases} \tag{25}$$

where $\xi > 1$ is an adaptive parameter chosen by designer; ε is a very small and positive parameter, $0 < \varepsilon << 1$, chosen by designer to avoid the singular cases of the expressions typed A/B.

Proof: By using the time derivative of (5) and $x^{(n)}$ from (2) with a note that in this phase, the controller is designed without any considered disturbance, the followings are given

$$\dot{S}(x) = \sum_{i=1}^{n-1} a_i e^{(i)} + x^{(n)} - x_d^{(n)}; \tag{26}$$

$$\dot{S}(x) = \sum_{i=1}^{n-1} a_i e^{(i)} + f(\mathbf{x},t) + g_1(\mathbf{x},t)u_s(t) - x_d^{(n)}. \tag{27}$$

From (14) and (27), the following expressions are obtained:

$$\begin{aligned}\dot{S}(x) =& \left(f(\mathbf{x},t) - \hat{f}(\mathbf{x},\boldsymbol{\varphi}_f)\right)\\ &+ \left(g_1(\mathbf{x},t) - \hat{g}_1(\mathbf{x},\boldsymbol{\varphi}_g)\right)u_s(t) - h(\mathbf{x},t);\end{aligned} \tag{28}$$

$$\begin{aligned}\dot{S}(x) =& \left(\hat{f}(\mathbf{x},\boldsymbol{\varphi}_f^*) - \hat{f}(\mathbf{x},\boldsymbol{\varphi}_f)\right)\\ &+ \left(\hat{g}_1(\mathbf{x},\boldsymbol{\varphi}_g^*) - \hat{g}_1(\mathbf{x},\boldsymbol{\varphi}_g)\right)u_s(t)\\ &- h(\mathbf{x},t) + \Omega(x,\boldsymbol{\varphi}_f,\boldsymbol{\varphi}_g);\end{aligned} \tag{29}$$

$$\begin{aligned}\dot{S}(\mathbf{x}) =& \boldsymbol{\psi}_f^T\boldsymbol{\lambda}(\mathbf{x}) + \boldsymbol{\psi}_g^T\boldsymbol{\lambda}(\mathbf{x})u_s(t) - h(\mathbf{x},t)\\ &+ \Omega(x,\boldsymbol{\varphi}_f,\boldsymbol{\varphi}_g),\end{aligned} \tag{30}$$

where

$$\boldsymbol{\psi}_f = \boldsymbol{\varphi}_f^* - \boldsymbol{\varphi}_f;\ \ \boldsymbol{\psi}_g = \boldsymbol{\varphi}_g^* - \boldsymbol{\varphi}_g. \tag{31}$$

By choosing a Lyaponov function as below

$$V_1 = \frac{1}{2}S(\mathbf{x})^2 + \frac{1}{2}\boldsymbol{\psi}_f^T\boldsymbol{\psi}_f + \frac{1}{2}\boldsymbol{\psi}_g^T\boldsymbol{\psi}_g, \tag{32}$$

with reference to (30) and (20), the following expressions are obtained:

$$\begin{aligned}\dot{V}_1 =& S(\mathbf{x})\left(\boldsymbol{\psi}_f^T\boldsymbol{\lambda}(x) + \boldsymbol{\psi}_g^T\boldsymbol{\lambda}(x)u_s(t) - h(\mathbf{x},t) + \Omega(\mathbf{x},\boldsymbol{\varphi}_f,\boldsymbol{\varphi}_g)\right)\\ &+ \boldsymbol{\psi}_f^T\dot{\boldsymbol{\psi}}_f + \boldsymbol{\psi}_g^T\dot{\boldsymbol{\psi}}_g;\end{aligned} \tag{33}$$

$$\begin{aligned}\dot{V}_1 =& \boldsymbol{\psi}_f^T\left(S(\mathbf{x})\boldsymbol{\lambda}(x) + \dot{\boldsymbol{\psi}}_f\right)\\ &+ \boldsymbol{\psi}_g^T\left(S(\mathbf{x})\boldsymbol{\lambda}(x)u_s(t) + \dot{\boldsymbol{\psi}}_g\right)\\ &- k_1 S(\mathbf{x})\operatorname{sat}\left(S(\mathbf{x})/\Phi\right)\left(1 - \exp\left(-k_2\left|S(\mathbf{x})\right|\right)\right)\\ &+ S(\mathbf{x})\left(\Omega(\mathbf{x},\boldsymbol{\varphi}_f,\boldsymbol{\varphi}_g)\right).\end{aligned} \tag{34}$$

In (34), due to

$$\begin{aligned}\dot{\boldsymbol{\psi}}_f &= \frac{d}{dt}\left(\boldsymbol{\varphi}_f^* - \boldsymbol{\varphi}_f\right) = -\dot{\boldsymbol{\varphi}}_f;\\ \dot{\boldsymbol{\psi}}_g &= \frac{d}{dt}\left(\boldsymbol{\varphi}_g^* - \boldsymbol{\varphi}_g\right) = -\dot{\boldsymbol{\varphi}}_g,\end{aligned} \tag{35}$$

hence,

$$\begin{aligned}\dot{V}_1 =& \boldsymbol{\psi}_f^T\left(S(\mathbf{x})\boldsymbol{\lambda}(x) - \dot{\boldsymbol{\varphi}}_f\right) + \boldsymbol{\psi}_g^T\left(S(\mathbf{x})\boldsymbol{\lambda}(x)u_s(t) - \dot{\boldsymbol{\varphi}}_g\right)\\ &- k_1 S(\mathbf{x})\operatorname{sat}\left(S(\mathbf{x})/\Phi\right)\left(1 - \exp\left(-k_2\left|S(\mathbf{x})\right|\right)\right)\\ &+ S(\mathbf{x})\left(\Omega(x,\boldsymbol{\varphi}_f,\boldsymbol{\varphi}_g)\right).\end{aligned} \tag{36}$$

If update law (24) is used, we have the following

$$\dot{V}_1 = -k_1 S(\mathbf{x})\operatorname{sat}\left(S(\mathbf{x})/\Phi\right)\left(1 - \exp\left(-k_2\left|S(\mathbf{x})\right|\right)\right)$$

$$+S(\mathbf{x})\,\Omega(x,\varphi_f,\varphi_g). \tag{37}$$

There are two cases related to (37) as below:

The first case, $|S/\Phi| > 1$, to which the followings can be inferred

$$\begin{aligned}\dot{V}_1 &= -k_1 S(\mathbf{x})\mathrm{sgn}\left(S(\mathbf{x})/\Phi\right)\left(1-\exp\left(-k_2\,|S(\mathbf{x})|\right)\right)\\ &\quad + S(\mathbf{x})\Omega(\mathbf{x},\varphi_f,\varphi_g),\\ \dot{V}_1 &= -k_1\,|S(\mathbf{x})|\left(1-\exp\left(-k_2\,|S(\mathbf{x})|\right)\right)\\ &\quad + S(\mathbf{x})\Omega(\mathbf{x},\varphi_f,\varphi_g),\\ \dot{V}_1 &< -k_1\,|S(\mathbf{x})|\left(1-\exp\left(-k_2\,|S(\mathbf{x})|\right)\right)\\ &\quad + |S(\mathbf{x})|\,\Omega_0.\end{aligned} \tag{38}$$

It means,

$$\dot{V}_1 < |S(\mathbf{x})|\left(\Omega_0 - k_1\left(1-\exp\left(-k_2\,|S(\mathbf{x})|\right)\right)\right). \tag{39}$$

So, it can infer the update law of $k_1(t)$ as follows:

$$\begin{aligned}k_1(t) =& \xi\frac{\Omega_0}{1-\exp(-k_2\,|S(\mathbf{x})|)+\varepsilon},\\ & \xi > 1,\ 0<\varepsilon << 1.\end{aligned} \tag{40}$$

The second case, $|S/\Phi| \le 1$, so expression (37) can be re-written as below:

$$\begin{aligned}\dot{V}_1 =& -k_1\frac{S(\mathbf{x})^2}{\Phi}\left(1-\exp\left(-k_2\,|S(\mathbf{x})|\right)\right)\\ & + S(\mathbf{x})\Omega(\mathbf{x},\varphi_f,\varphi_g),\end{aligned}$$

to which we have:

$$\begin{aligned}\dot{V}_1 &< -k_1\frac{S(\mathbf{x})^2}{\Phi}\left(1-\exp\left(-k_2\,|S(\mathbf{x})|\right)\right) + |S(\mathbf{x})|\,\Omega_0\\ &= |S(\mathbf{x})|\left(-k_1\frac{|S(\mathbf{x})|}{\Phi}\left(1-\exp\left(-k_2\,|S(\mathbf{x})|\right)\right)+\Omega_0\right).\end{aligned} \tag{41}$$

Based on (41), the update law of $k_1(t)$ when $|S/\Phi| \le 1$ is inferred as in (42).

$$\begin{aligned}k_1(t) =& \xi\frac{\Omega_0\Phi}{(|S(\mathbf{x})|+\varepsilon)(1+\varepsilon-\exp(-k_2\,|S(\mathbf{x})|))}\\ & \xi > 1,\ 0<\varepsilon << 1.\end{aligned} \tag{42}$$

Deriving from (40) and (42), we have the update law given in (25). □

4. DESIGNING THE DO-FSMC

The proposed DO-FSMC is employed for a class of SISO n-th order nonlinear systems subjected to UAD. The DO-FSMC is constituted of the DO and FSMC.

4.1. Building the DO

As mentioned in Remark 2, the DO based on the known functions $f_0(.)$, $g_{01}(.)$ and $g_{02}(.)$ of (1) to estimate $d(t)$. By replacing $f(.)$, $g_1(.)$ and $g_2(.)$ in (2) with $f_0(.)$, $g_{01}(.)$ and $g_{02}(.)$, Equation (2) can be re-written in the form of (43):

$$\begin{cases}\dot{x}_1 = x_2,\\ \quad\vdots\\ \dot{x}_{n-1} = x_n,\\ \dot{x}_n = x^{(n)} = f_0(\mathbf{x},t) + g_{01}(\mathbf{x},t)u(t) + g_{02}(t)d(t),\\ y = x,\end{cases} \tag{43}$$

or in the simple form as in (44),

$$\begin{cases}\dot{\mathbf{x}} = F(\mathbf{x},t) + G_1(\mathbf{x},t)u(t) + G_2(\mathbf{x},t)d(t),\\ y = x,\end{cases} \tag{44}$$

where

$$F(\mathbf{x},t) = [x_2,\ x_3,...,\ x_n, f_0(\mathbf{x},t)]^{\,T} \in R^n, \tag{45}$$

$$G_1(\mathbf{x},t) = [0,...,0,\ g_{01}(\mathbf{x},t)]^{\,T} \in R^n, \tag{46}$$

$$G_2(\mathbf{x},t) = [0,...,0,\ g_{02}(t))]^{\,T} \in R^n. \tag{47}$$

Let $\hat{d}(t)$ be the estimate of $d(t)$. By using the method presented in [35], $\hat{d}(t)$ is expressed as:

$$\hat{d}(t) = z(\mathbf{x},t) + p(\mathbf{x}), \tag{48}$$

in which $z(\mathbf{x},t)$is the internal state of the nonlinear observer. Function $z(\mathbf{x},t)$ is estimated via the following expression:

$$\begin{aligned}\dot{z}(\mathbf{x},t) =& -l(\mathbf{x})\left(G_1(\mathbf{x},t)u(t) + G_2(\mathbf{x},t)p(\mathbf{x}) + F(\mathbf{x},t)\right)\\ & - l(\mathbf{x})G_2(\mathbf{x},t)z(\mathbf{x},t),\end{aligned} \tag{49}$$

where $p(\mathbf{x})$ is a designed nonlinear function, and $l(\mathbf{x}) = \partial p/\partial \mathbf{x}$ is a vector which needs to be determined so that the error function (50) converges to zero.

$$E(t) = d(t) - \hat{d}(t). \tag{50}$$

For this application, attributes of the DO are expressed by the following theorem:

Theorem 2: Let's consider system (2) which is re-written as in (44). It is assumed that the time varying rate of disturbances impacting on the system is slow. If the estimate $\hat{d}(t)$ depicted in (48) is used with$l(\mathbf{x}) = [l_1,...,l_n]$, then $\forall l_i \in \Re$, $i = 1,\ ...,\ n$, ($\Re$: the real number set) and $l_n > 0$, the $E(t) \to 0$ when $t \to \infty$ is a stable process.

Proof: With taking notes of (48), (49) and $l(\mathbf{x}) = \partial p/\partial x$, the time derivative of (50) is obtained as follows:

$$\dot{E}(t) = \dot{d}(t) - \dot{\hat{d}}(t) = \dot{d}(t) - \dot{z}(\mathbf{x},t) - \frac{\partial p}{\partial \mathbf{x}}\dot{\mathbf{x}}, \tag{51}$$

$$\dot{E}(t) = \dot{d}(t) - \dot{z}(\mathbf{x},t) - l(\mathbf{x})\dot{\mathbf{x}}. \tag{52}$$

From (52) and (44), the following result is obtained

$$\begin{aligned}\dot{E}(t) =& \dot{d}(t) - \dot{z}(\mathbf{x},t) \\ & - l(\mathbf{x})\left(F(\mathbf{x},t) + G_1(\mathbf{x},t)u(t) + G_2(\mathbf{x},t)d(t)\right).\end{aligned} \tag{53}$$

By substituting $\dot{z}(\mathbf{x},t)$ from (49) into (53) with taking note of (50) we have

$$\begin{aligned}&\dot{E}(t) = \dot{d}(t) + l(\mathbf{x})G_2(\mathbf{x},t)\left(z(\mathbf{x},t) + p(\mathbf{x}) - d(t)\right), \\ &\dot{E}(t) = \dot{d}(t) - l(\mathbf{x})G_2(\mathbf{x},t)E(t).\end{aligned} \tag{54}$$

If the time varying rate of the uncertainty aspects is low, (54) can be rewritten as in (55).

$$\dot{E}(t) + l(\mathbf{x})G_2(\mathbf{x},t)E(t) \approx 0. \tag{55}$$

In this expression, $l(\mathbf{x})$ is a vector of polynomials with respect to the state variable$x$. Simply, we chose it as a row vector of constant coefficients as below:

$$l(\mathbf{x}) = [l_1, ..., l_n], \quad l_i \in \Re,\ i = 1...n. \tag{56}$$

Deriving from (47) and (56) we have (57):

$$\dot{E}(t) + l_n g_{02}(t)E(t) \approx 0. \tag{57}$$

Due to $g_{02}(t) > 0$, it can observe from (57) that $l_n > 0$ is the sufficient condition to guarantee that $E(t) \to 0$ or $\hat{d}(t) \to d(t)$ when $t \to \infty$. It means that $\forall l_i \in \Re$, $i = 1$, ..., n, and $l_n > 0$, $E(t) \to 0$ is a stable process. □

From Theorem 2, the estimate of $d(t)$ can be established via the DO as below:

$$\begin{aligned}&\hat{d}(t) = z(x,t) + p(\mathbf{x}), \\ &p(\mathbf{x}) = \sum_{i=1}^{n} l_i x_i,\ l_i \in \Re,\ i = 1, ..., (n-1),\ l_n \in \mathrm{N}*, \\ &\dot{z}(\mathbf{x},t) = -l_n g_{02}(t)z(x,t) - l(\mathbf{x})\bar{K},\end{aligned}$$

where $l(\mathbf{x}) = [l_1, ..., l_n]$ and

$$\bar{K} = \begin{bmatrix} x_2 \\ x_3 \\ \vdots \\ x_n \\ g_{01}(\mathbf{x},t)u(t) + g_{02}(t)p(\mathbf{x}) + f_0(\mathbf{x},t) \end{bmatrix}.$$

Remark 4: Related to vector $l(\mathbf{x})$ (56), if we take only interest in the stable condition of the process $E(t) \to 0$ or $\hat{d}(t) \to d(t)$ when $t \to \infty$, the ties $l(\mathbf{x}) = [0, ..., 0, l_n] \in R^n$ and $l_n > 0$ are appropriate options. If we consider both, the stable condition and optimal solution, the ties $\forall l_i \in \Re$, $i = 1$, ..., $(n-1)$ and $l_n > 0$ as abovementioned should be utilized. The larger value of l_n makes the convergence rate increase but may result in growing rapidly the POT (percentage of overshoot). Hence, a reasonable value of this one needs to be considered.

4.2. The DO-FSMC

The DO-FSMC is constituted of the FSMC and DO. The control signal $u(t)$ created by the DO-FSMC is $u(t) = u_s(t) + u_c(t)$ as in (3), where $u_s(t)$ comes from the FSMC while $u_c(t)$ is determined based on the DO. Theorem 3 as below analyzes stability attribute of this combination.

Theorem 3: Consider control system (2) subjected to disturbance $d(t)$ whose time varying rate is slow. The system controlled by the DO-FSMC via control law (58) as below:

$$u(t) = u_s(t) - \frac{g_2(t)}{g_{01}(t)}\hat{d}(t), \tag{58}$$

where $u_s(t)$ is specified via Theorem 1; $\hat{d}(t)$ is determined via Theorem 2. Then $e(t) \to 0$ (or $x \to x_d$) of the system when $t \to \infty$ is an asymptotically stable process, in which $e(t)$ is the error vector defined in (4).

Proof: In order to analyze dynamic response feature of system (2) subjected to disturbance, we again utilize the sliding surface $S(\mathbf{x})$ (5) and Lyapunov candidate function $V_0(x)$ (6). With reference to (7), (8) and taking notes of $V_0(0) = 0$ and $V_0(x) \geq 0\ \forall x(t) | t > 0$, in view of Lyapunov stability we can infer that if the control law $u(t)$ is employed such that $\dot{S}(x) = -\rho\,\mathrm{sgn}\left(S(\mathbf{x})\right)$, then $S(\mathbf{x}) \to 0$ is an asymptotically stable process. Hence, from (8), (10), (5), (4) and (2), the feedback control signal such that $e(t) \to 0$ or $x \to x_d$ when $t \to \infty$ is a stable Lyaponov process can be inferred as below:

$$\begin{aligned}u(t) =& \frac{1}{g_1(\mathbf{x},t)}\left(-\sum_{i=1}^{n-1} a_i e^{(i)} - f(\mathbf{x},t) + x_d^{(n)} - h(\mathbf{x},t)\right) \\ & - d(t)g_2(t)\big/g_1(\mathbf{x},t) = A + B.\end{aligned} \tag{59}$$

Be noted that in (59), $B = -d(t)g_2(t)\big/g_1(\mathbf{x},t)$ reflects the impact of disturbance on the system. By compensating for disturbance with a value of $u_c(t) = B$, this influence can be seen as being exterminated. Thus, we can deal then with system (2) as a system without disturbance. It means that, by using $h(\mathbf{x},t)$ from (20), replacing $g_1(\mathbf{x},t)$ and $f(\mathbf{x},t)$ in the expression A with fuzzy approximate functions $\hat{g}_1(\mathbf{x},t)$ and $\hat{f}(\mathbf{x},t)$ from (17) as well as adopting the update laws (24) and (25), the remainder of (59), A, becomes the output signal $u_s(t)$ (14) of the FSMC which has been designed for system (2) without disturbance presented in Theorem 1.

To quantify the compensation part $u_c(t)$, instead of $g_1(\mathbf{x},t)$ and $d(t)$ we employ function $g_{01}(t)$ in (1) and the estimate value $\hat{d}(t)$ of the DO which is obtained from Theorem 2. Thus, $u_c(t)$ is as follows:

$$u_c(t) = -\frac{g_2(t)}{g_{01}(t)}\hat{d}(t). \tag{60}$$

It should be noted in (60) that $g_2(t)$ is the known function; $g_{01}(t) \approx g_1(\mathbf{x},t)$; while the stability of the process $\hat{d}(t) \to d(t)$ when $t \to \infty$ has been proved in Theorem 2.

As a result of the above approach, equation (59) becomes (58). It should be also noted that (59) and (58) are the two control laws for system (2) with disturbance. Due to, as mentioned above, controlled by (59), the process $\mathbf{e}(t) \to 0$ when $t \to \infty$ to be asymptotically stable, it can imply that controlled by the DO-FSMC via (58), dynamic response of system (2) subjected to disturbance is also an asymptotically stable process. □

Remark 5: Related to the design of the DO-FSMC, the followings can be implied from Theorems 1-3. Due to the functions of the DO and FSMC to be independent, since, for simplicity, the design of these two parts can be performed individually. When they take part in the controller DO-FSMC, the stability of the closed loop system will be guaranteed by the close tie established via the control law (58). Besides, the ability to stably converge to zero of the DO reflected in Theorem 2 as well as the stability attribute of the FSMC presented in Theorem 1 contribute positively to the effectiveness of the DO-FSMC.

5. A TECHNIQUE SYSTEM BASED ON THE PROPOSED METHOD

In this section, a quarter car MRD suspension model shown in Fig. 1 is used to verify the proposed DO-FSMC via two groups, the simulation surveys as well as the real surveys based on an experimental apparatus as in Figs. 8 and 9.

For comparing, four other suspension systems established based on the structure in Fig. 1 are also utilized. The first one is controlled by the controller using an adaptive neuro-fuzzy inference system (ANFIS), sliding mode control, and disturbance and uncertainty observer named NFSmUoC [30]. The second one is an adaptive T-S fuzzy sliding control system called the K controller [36]. The third one is a fuzzy-based predicting sliding controller (FPSC) for active railway suspension systems subjected to UAD [37]. The fourth one is the passive suspension system (uncontrolled). It should be noted that the five systems have the similar structures (the MRD Suspension) as in Fig. 1; the only difference relates to the controller. Features of them are shown in Table 1.

Dynamic response results of the chassis mass are used to estimate the proposed theory. To show quantitative results, the maximum magnitude of chassis displacement and acceleration A_d, $A_a$as below will be used,

$$A_d = \max_{i=1\ldots P} \left|z_s^i\right|; \; A_a = \max_{i=1\ldots P} \left|\ddot{z}_s^i\right|. \tag{61}$$

In these, P is the number of samples used for the survey; z_s and $\ddot{z}_s$, respectively, are the vertical displacement and acceleration of the chassis.

5.1. Describing the system

The structure of the technique system has three main parts. The first one is the suspension using a magnetorheological damper (MRD), a damper with the damping coefficient c_s, and a linear spring with the stiffness coefficient k_s. The second one is the controller which is used to control the MRD. The third one is the inverse MRD using an ANFIS named ANFIS-I-MRD (see [30]). In this surveys, $m_s(t)$ consists of chassis mass (also called to be the sprung mass) including the load, passengers and impacting from surrounding environment such as the wind force. This is the time varying parameter. The constant parameter m_u expresses the unsprung mass. The vertical displacement of the sprung and unsprung mass are signed to be $z_s(t)$ and $z_u(t)$, respectively, while that of the road profile is signed $z_r(t)$. In this case, we assume that the ability to hold road is good enough, so $z_u(t) = z_r(t)$.

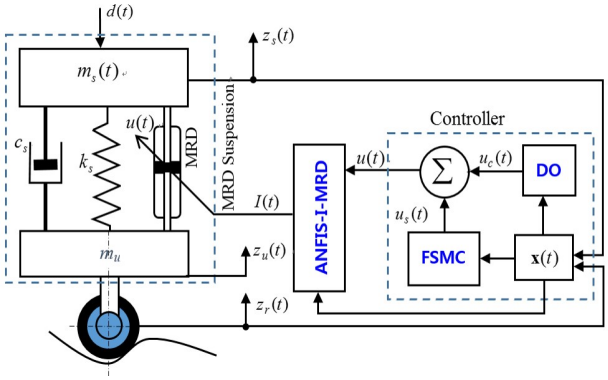

Fig. 1. The structure and operating principle of the semi-active MRD suspension system 1 DOF.

Table 1. Special features of each suspension system.

Systems	Detailed
Passive	Uncontrolled
NFSmUoC	- UAD are estimated simultaneously; - Using SMC only to determine $u_s(t)$.
DO-FSMC	- UAD are estimated separately; - Using FL and SMC to estimate $u_s(t)$.
K	- T-S fuzzy model is used to depict the system and compensate for uncertainty; - FL and SMC are used for setting up the control law.
FPSC	- UAD is estimated simultaneously; - Using ANFIS for predicting road status; - FL and SMC are used for setting up the control law.

When the system operates, the chassis mass is forced to vibrate due to vertical vibration of the wheel. In order to stamp out chassis vibration, the required current $I(t)$ estimated by the controller is used to control the MRD to generate required damping force $u(t)$ such that vibration of the chassis mass m_s is reduced. Related to this work, the ability of the controller is depicted via the corresponding dynamic response coming from the chassis vibration.

Be noted here that it is different from the real sur-

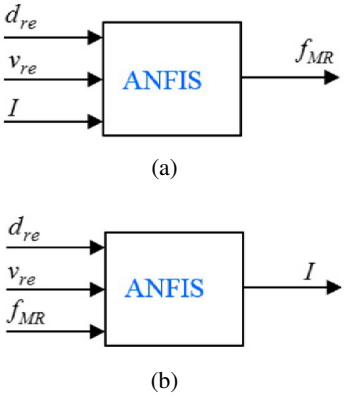

Fig. 2. Operating diagram of the AMFIS-D-MRD (a) and ANFIS-I-MRD (b).

Table 2. Parameters of the suspension.

$m_s = 19600 \pm 4000$	kg
$m_u = 1440$	kg
$k_s = (392 \pm 10).10^4$	N/m
$c_s = 53900 \pm 2000$	Ns/m

veys presented in Subsection 5.4, for the simulations in Subsection 5.3, the MRD is replaced by its direct model named ANFIS-D-MRD created by an ANFIS and a measured data set. In order to build the ANFIS-I-MRD and ANFIS-D-MRD, the algorithm for building ANFIS from a data set named B-ANFIS presented by Nguyen *et al.* [1] and measured data sets expressing dynamic response of a MRD are used. The operating diagrams of these models are depicted in Fig. 2, where d_{re} and v_{re} respectively are relative piston-cylinder displacement and velocity of the MRD; I is current supporting the MRD while f_{MR} is the damping force generated by the MRD. In these simulation surveys, the disturbance status is expressed by the random changing of the chassis mass, $m_s = 19600 \pm 4000$; while the uncertainty status is depicted by the random changing of $k_s$andc_s as follows: $k_s = (392 \pm 10) \cdot 10^4$, $c_s = 53900 \pm 2000$ as in Table 2.

5.2. Establishing the DO-FSMC for the suspension

5.2.1 The FSMC for the suspension

The state space is expressed via the dynamic response of the sprung mass as follows:

$$\mathbf{x}(t) = [x_1,\ x_2]^T = [z_s,\ \dot{z}_s]^T. \tag{62}$$

Based on Fig. 1, the spring and damping force as well as dynamic response of the sprung mass are expressed as follows:

$$f_s = k_s(x_1 - z_r), f_d = c_s(x_2 - \dot{z}_r), \tag{63}$$

Table 3. Parameters of the FSMC.

Sliding surface	$S = 10e + \dot{e}$
k_2	1.5
ξ	2
ε	0.01
Φ	1
$x_d = [x_1, x_2]^T = [z_s, \dot{z}_s]^T$	$[0,\ 0]^T$
Number of fuzzy laws	49

$$\begin{cases} m_s(t)\ddot{z}_s + k_s(x_1 - z_r) + c_s(x_2 - \dot{z}_r) = -u(t) + d(t), \\ y = z_r. \end{cases} \tag{64}$$

From (64), the equations typing (1) expressing the suspension system is depicted as in (65).

$$\begin{cases} z_s^{(2)} = f_0(\mathbf{x},t) + g_{01}(\mathbf{x},t)\,u(t) + g_{02}(t)D(t), \\ y = x_1, \end{cases} \tag{65}$$

where

$$f_0(\mathbf{x},t) = -\frac{1}{m_s(t)}\left(k_s(x_1 - z_r) + c_s(x_2 - \dot{z}_r)\right), \tag{66}$$

$$g_{01}(\mathbf{x},t) = -1/m_s(t), \tag{67}$$

$$g_{02}(t) = 1/m_s(t). \tag{68}$$

The equations typing (2) expressing the suspension system are as in (69).

$$\begin{cases} z_s^{(2)} = f(\mathbf{x},t) + g_1(\mathbf{x},t)\,u(t) + g_2(t)d(t), \\ y = x_1, \end{cases} \tag{69}$$

where $g_2(t) = g_{02}(t) = 1/m_s(t)$.

Related to the control law of the FSMC, parameters are chosen as in Table 3.

5.2.2 The DO for the suspension

Deriving from (43)-(47), (62) and (65)-(68), the followings are obtained

$$\dot{\mathbf{x}} = \begin{bmatrix} \dot{x}_1 \\ \dot{x}_2 \end{bmatrix} = F(\mathbf{x},t) + G_1(\mathbf{x},t)u(t) + G_2(t)d(t), \tag{70}$$

where

$$\begin{aligned} F(x,t) &= [x_2,\ f_0(\mathbf{x},t)]^T \\ &= \left[x_2,\ -\left(k_s(x_1 - z_r) + c_s(x_2 - \dot{z}_r)\right)/m_s(t)\right]^T, \end{aligned} \tag{71}$$

$$G_1(\mathbf{x},t) = [0,\ g_{10}(\mathbf{x},t)]^T = \left[0,\ -1/m_s(t)\right]^T, \tag{72}$$

$$G_2(\mathbf{x},t) = [0,\ g_{20}(t)]^T = \left[0,\ 1/m_s(t)\right]^T. \tag{73}$$

Hence, based on Theorem 2, the followings are given

$$l(\mathbf{x}) = [l_1,\ l_2];\ p(\mathbf{x}) = l_1x_1 + l_2x_2, \tag{74}$$

Table 4. Parameters of the DO.

l_1	1.51
l_2	24.4

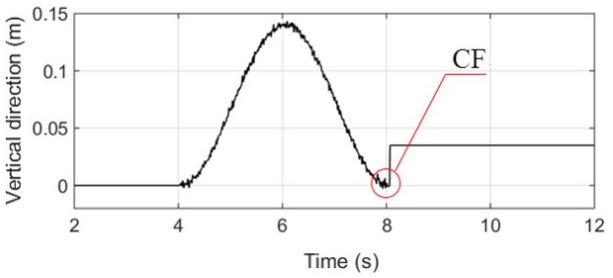

Fig. 3. The bump road profile is used for surveys.

$$\dot{z}(\mathbf{x},t) = -l_2 g_{02}(t) z(\mathbf{x},t) - l(\mathbf{x})\bar{K}, \tag{75}$$

$$\bar{K} = \begin{bmatrix} x_2 \\ g_{01}(\mathbf{x},t)u(t) + g_{02}(t)p(\mathbf{x}) + f(\mathbf{x},t) \end{bmatrix}. \tag{76}$$

Value of $[l_1,\ l_2]$ used in this paper is in Table 4.

5.3. Simulation surveys

In this subsection, the rough bump road with a cross fracture (CF) as in Fig. 3 is used as $z_r(t)$ in the system expressed in (64). The passive suspension and the suspensions controlled by the DO-FSMC and NFSmUoC are all used.

The road profile as in Fig. 3 is mathematically described as below:

$$x_0(t) = \begin{cases} X_0\,(1-\cos(\omega_r t)) & \text{if } 2\pi/\omega_r \le t \le 4\pi/\omega_r, \\ 0 & \text{if } \quad t < 2\pi/\omega_r, \\ X_0 - A_0 & \text{if } \quad t > 4\pi/\omega_r, \end{cases} \tag{77}$$

where $\omega_r = 2\pi V_c/D$; X_0 ($= 0.07$ m) is the haft of the bump height; A_0 is a parameter which is 0.035 m in this paper; D ($= 1.4$ m) is the width of the bump; V_c is the vehicle velocity. In the test, the vehicle is assumed to travel the bump with a constant velocity of 25 km/h ($V_c = 6.944$ m/s). The objective of the control system is to support the damping force $u(t)$ such that vibration of the chassis mass is stamped out as soon as possible. This means the desired $x_d = [x_1,\ x_2]^T = [z_s,\ \dot{z}_s]^T = [0,\ 0]^T$.

The results obtained from the passive, NFSmUoC and DO-FSMC suspensions are shown in Figs. 4-7 and Table 5.

Fig. 4 and Table 5 show that the smallest displacement belongs the suspension system controlled by the DO-FSMC. The maximum displacement magnitudes corresponding to the passive, NFSmUoC, and DO-FSMC, respectively, are 0.1014, 0.0261 and 0.0179 (m).

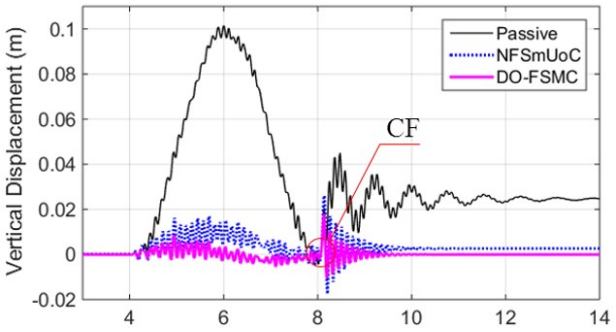

Fig. 4. Vertical displacement of the chassis mass corresponding to the three systems.

Table 5. The maximum magnitudes.

	A_d (m)	A_a (m/s^2)
Passive	0.1014	6.4573
NFSmUoC	0.0261	0.8913
DO-FSMC	0.0179	0.4649

The other features can be seen at the cross fracture (CF) and during the next period in Fig. 4. Namely, for the controlled systems, the output is stable after about 2 seconds while that of the passive is more than 6 seconds. Besides, in this area, the stable value of the state variable$x_1(t)$ corresponding to the proposed controller is $1.5864 \cdot 10^{-4}$ (m) which is smaller than that of the NFSmUoC to be 0.0026 (m). For the passive system, the system could not get the desired value. It is stable at the larger value which is 0.35 (m). Be noted here that the required value of chassis displacement is $x_{1d} = 0$(m). This shows that the ability to get the x_{1d} of the DO-FSMC is quite good, better than the NFSmUoC and much better than the passive.

The competence to stamp out vibration of the DO-FSMC is also clearly represented via the vertical acceleration of the chassis mass. Fig. 5 and Table 5 show that the maximum acceleration magnitudes at CF corresponding to the DO-FSMC, NFSmUoC and the passive one are 0.4649, 0.8913 and 6.4573 (m/s^2).

Related to the damping force generated by the controller DO-FSMC, this can be seen in Figs. 6 and 7. The positive results mentioned above of the proposed method relate to the compensated force part $u_c(t)$ generated by the DO as in Fig. 6 and the damping force, in total, $u(t) = u_c(t) + u_s(t)$ as in Fig. 7. The controller DO-FSMC could generate the control force appropriate and large enough to stamp out chassis vibration.

5.4. Surveys via an experimental setup

In this subsection, the experimental apparatus shown in Fig. 8 and detailed in Fig. 9 is used to again verify the competence of the DO-FSMC to control the quarter vehicle MRD suspension, a real system.

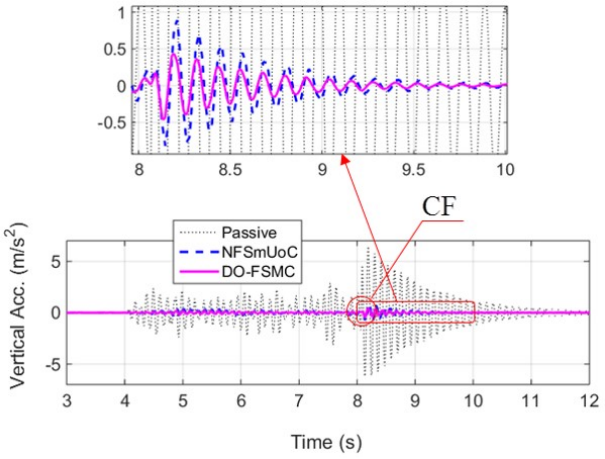

Fig. 5. Vertical acceleration of the chassis mass.

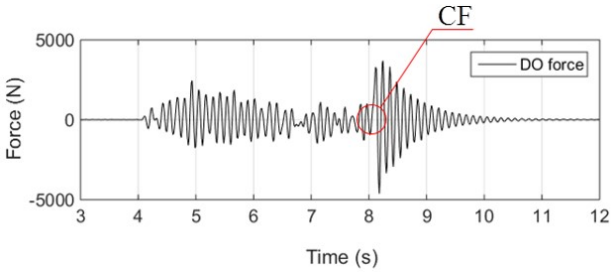

Fig. 6. Damping force $u_c(t)$ compensated by the DO.

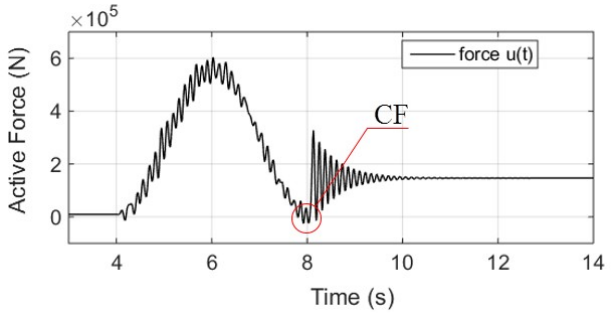

Fig. 7. Damping force in total generated by the controller DO-FSMC.

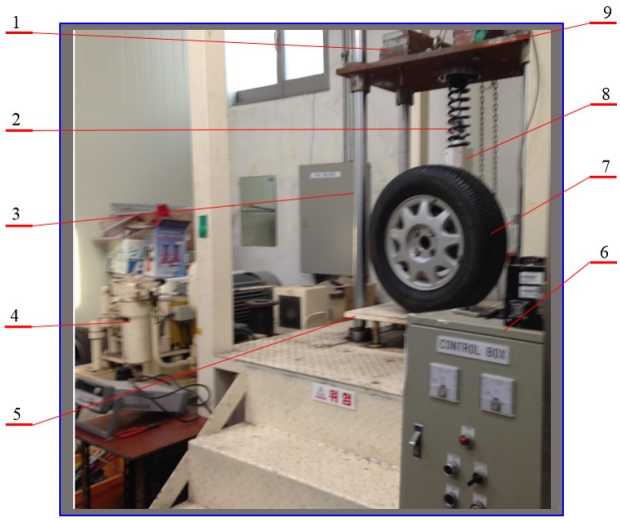

Fig. 8. The experimental setup used for evaluating the DO-FSMC.

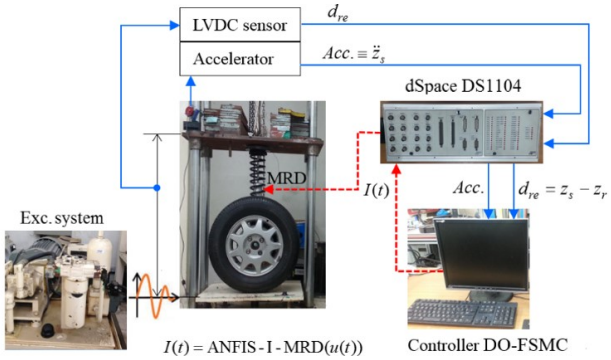

Fig. 9. The structure and operating of the experimental apparatus mentioned in Fig. 9 for evaluating the DO-FSMC.

Table 6. The main parameters of the suspension system.

$m_s = 246.5 \pm 25$	kg
$k_s = 2.8.10^4$	N/m
$c_s = 3000$	Ns/m

The experimental apparatus consists of four main equipment groups as follows: 1) The suspension system is constituted of the linear spring $k_s = 2.8 \cdot 10^4$ N/m (2) and the MRD with a damping coefficient of $c_s = 3000$ Ns/m corresponding to the zero current (8). 2) The hydraulic excitation system is operated by the hydraulic unit (4) connected to the lower bed (5). 3) The mechanical structure is constituted of the upper bed (9), lower bed and four parallel vertical circle pillars (3) which is used to fix the suspension system, wheel (7), unsprung mass (1) and sensors. 4) The control system consists of a computer, an AD/DA converter, an amplifier, sensors and so on (6). In this survey, the unsprung mass is $m_s = 246.5 \pm 25$ kg including the mass of (9). Table 6 lists the main parameters of the system.

The excitation from (4) results in displacement of the lower bed which makes the unsprung mass vibrate vertically freely along the pillars (3) via the wheel and suspension. The relative displacement between the sprung and unsprung mass is measured by a LVDT (linear variable differential transformer), while acceleration of the unsprung mass is measured by an accelerometer. The signal from the sensors transmits to the computer via the AD converter. Conversely, the control signal from the computer transmits to the MRD via the DA converter and am-

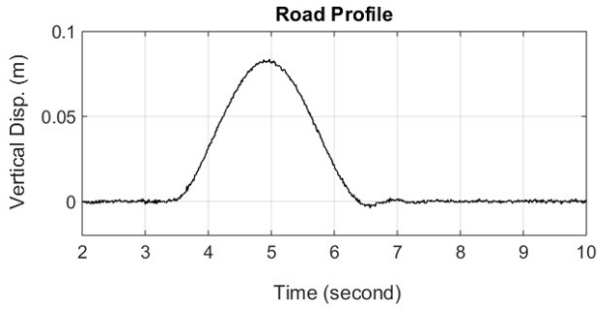

Fig. 10. Vertical displacement measured at the lower bed which participates as the road profile impacting on the suspension systems.

plifier. The role of the AD/DA converter is to transform the signal from analog to digital and conversely, while the amplifier is used to generate the control current supporting the MRD to apply the required active force which is determined from the control algorithms.

Based on this experimental setup, five suspension systems are established. Namely, by supporting the zero current during the operating time we have the passive suspension system. Another way, if the control current for the MRD determined from the controllers, the four corresponding semi-active MRD suspension systems are given. The road profile impacting directly on these suspensions is set up as follows: At the initial location of the lower bed, by controlling the hydraulic unit to apply a vertical displacement of the lower bed and return it to the initial location, the bump-typed road profile is described which is shown in Fig. 10 via the signal measured at the lower bed.

In this survey, obtained results from the suspensions are shown in Tables 7 and 8 and Figs. 11 and 12. The qualitative view can be seen in Fig. 11 that the acceleration of the suspension controlled by the controller DO-FSMC is the smallest. One of the main factors contributing to this positive result derives from the control force created by the proposed controller as in Fig. 12(a), by which the value of the sliding surface is remained quite small and stable as illustrated in Fig. 12(b). The quantitative results in Table 7 show that the maximum acceleration magnitude related to the controller DO-FSMC is 0.0910 m/s^2. It is smaller than that to be 0.1096, 0.1368, 0.1087 m/s^{2}coming from NFSmUoC, K, FPSC, respectively, and much smaller than that to be 0.2406 m/s^{2}from the passive one.

5.5. Discussion

For the simulations, forced by the control force determined by the DO-FSMC as in Figs. 6 and 7, the state variable $x_1(t)$ reached the desired state, $x_1(t) \to x_{1d}(t) = 0$, quickly and stably as in Fig. 4. At CF, control force is the largest and then, it is reduced corresponding to the decrease in $x_1(t)$. However, in order to keep $x_1(t) = 0$,

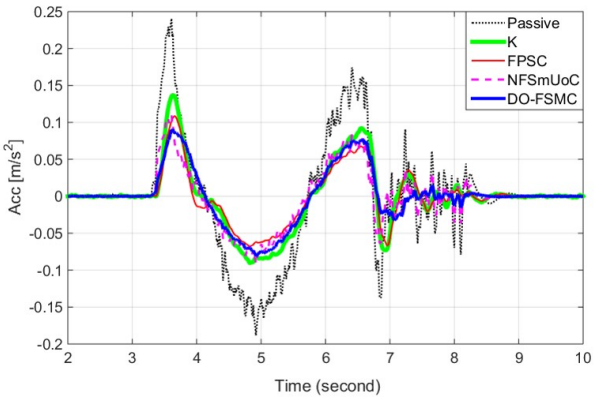

Fig. 11. Acceleration of the sprung mass$m_s$corresponding to the five systems.

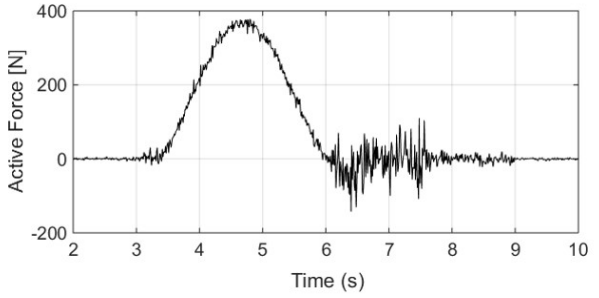

(a)

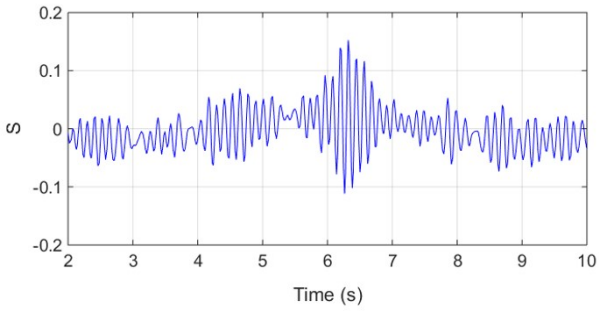

(b)

Fig. 12. The required damping force in total determined by the controller DO-FSMC and the attainability of the sliding mode surface, $S = S(x(t))$.

Table 7. The maximum acceleration magnitudes.

	A_a (m/s^2)
Passive	0.2406
NFSmUoC	0.1096
DO-FSMC	0.0910
K	0.1368
FPSC	0.1087

$u_s(t) > 0$ during the next period. For the real survey via the experimental setup, the above observation is much

Table 8. The relative acceleration-reduction coefficient.

	ζ_a	
	Simulation Survey	Experimental Survey
NFSmUoC	0.8620	0.5445
DO-FSMC	0.9280	0.6218

the same as the acceleration varying status of the sprung mass shown in Fig. 11. The control force determined by the DO-FSMC impacts efficiently on the chassis mass to stamp out its vibration as soon as possible. As a result, in these five suspensions, the setting time of the acceleration signal deriving from the one controlled by the DO-FSMC is shortest.

An issue, however, can be seen in Table 8 via ζ_a which is called the relative acceleration-reduction coefficient defined as follows:

$$\zeta_a = 1 - A_{ac}/A_{ap}, \tag{78}$$

where A_{ac} is the maximum acceleration magnitude (61) of m_s in the considered suspension system (the NFSmUoC or DO-FSMC) while A_{ap} is the maximum acceleration magnitude (61) of m_s in the passive suspension when the excitation conditions are similar. By using (78) and the results in Tables 5 and 7, we obtained the results in Table 8. This table shows that, together with the observation that the DO-FSMC is more efficient than the NFSmUoC as abovementioned, a negative aspect can be seen here that ζ_a of the controllable suspensions in the experimentally real survey (called Case 1) is always smaller than that deriving from the simulation survey (called Case 2). For example, controlled by the NFSmUoC, ζ_a in Case 1 to be 0.5445 is smaller than that in Case 2 to be 0.8620; similarly, controlled by the DO-FSMC, ζ_a in Case 1 to be 0.6218 is smaller than 0.9280 corresponding to Case 2.

The main reason of the fact that ζ_a deriving from the real system survey is always much smaller than that from the corresponding simulation survey is the time delay, signed τ. There are many causes resulting in τ. In these, the response delay of the equipment added to the passive system to establish the controllable suspensions such as the sensors, AD/DA converter, amplifier, MRD, and the calculating cost related to control programs are two main causes of this delay status.

6. CONCLUSION

The new design of fuzzy sliding mode control enhanced by compensation for UAD using a disturbance observer DO, named the DO-FSMC, has been presented. The method is employed for a class of SISO n-th order nonlinear control systems subjected to UAD, in which uncertainty comes from the model error while disturbance relates to external noise whose time-varying rate is low. The stability of the FSMC and DO-FSMC along with the convergence of the DO have been theoretically proved. The simulations as well as the surveys based on the semi-active suspension system using the MRD with measured datasets have been performed. These works showed that theoretically proved conclusions coincided with the obtained corresponding survey results. The semi-active smart suspension controlled by the DO-FSMC could stably reach the desired state in a short time, even in the poor area of the road profile, the cross fracture CF. Compared with the other, chassis mass acceleration of the one controlled by the DO-FSMC is the smallest.

It is finally remarked that for the real applications, the TVR of $d(t)$ may be high; besides, the time delay always exists and impacts negatively on the control effectiveness. The method, hence, needs to be expanded to deal with these issues. Designing delay compensators together with improving the capability to adapt to the higher TVR of $d(t)$ should be considered. These are as a second phase of this work.

REFERENCES

[1] S. D. Nguyen, Q. H. Nguyen, and S. B. Choi, "Hybrid clustering based fuzzy structure for vibration control - Part 1: a novel algorithm for building neuro-fuzzy system," *Mechanical Systems and Signal Processing*, vol. 50-51, pp. 510-525, 2014. [click]

[2] S. D. Nguyen, Q. H. Nguyen, and S. B. Choi, "Hybrid clustering based fuzzy structure for vibration control - Part 2: an application to semi-active vehicle seat-suspension system," *Mechanical Systems and Signal Processing*, vol. 56-57, pp. 288-301, 2014.

[3] J. Wang, A. B. Rad, and P. T. Chan, "Indirect adaptive fuzzy sliding model control - Part I: fuzzy switching," *Fuzzy Sets and Systems*, vol. 122, pp. 21-30, 2001. [click]

[4] O. Yakut and H. Alli, "Neural based sliding-mode control with moving sliding surface for the seismic isolation of structures," *J. of Vib. and Control*, vol. 17, pp. 2103-2116, 2011.

[5] X. Lingfei and Z. Yue, "Sliding-mode output feedback control for active suspension with nonlinear actuator dynamics," *Journal of Vibration and Control*, vol. 21, no. 14, 2015.

[6] H. L. Xing, D. H. Li, J. Li, and C. H. Zhang, "Linear extended state observer based sliding mode disturbance decoupling control for nonlinear multivariable systems with uncertainty," *Inter. Journal of Control, Automation and Systems*, vol. 14, no. 4, pp. 967-976, 2016. [click]

[7] R. Madoński and P. Herman, "Survey on methods of increasing the efficiency of extended state disturbance observers," *ISA Transactions*, vol. 56, pp. 18-27, 2015. [click]

[8] L. Wu, C. Wang, and Q. Zeng, "Observer-based sliding mode control for a class of uncertain nonlinear neutral delay systems," *Journal of the Franklin Institute*, vol. 345, pp. 233-253, 2008. [click]

[9] A. B. Sharkawy and S. A. Salman, "An adaptive fuzzy sliding mode control scheme for robotic systems," *Intel. Control and Auto.*, vol. 2, pp. 299-309, 2011.

[10] S. Bououden, M. Chadli, and H. R. Karimi, "Fuzzy sliding mode controller design using Takagi-Sugeno modelled nonlinear systems," *Hindawi Publishing Corporation Mathematical Problems in Engineering*, vol. 2013, Article ID 734094, p. 7, 2013.

[11] D. Ginoya, P. D. Shendge, and S. B. Phadke, "Disturbance observer based sliding mode control of nonlinear mismatched uncertain systems," *Comm. in Nonlinear Science and Num. Simu.*, vol. 26, pp. 98-107, 2015.

[12] H. Zhang, Y. Wang, and D. Liu, "Delay-dependent guaranteed cost control for uncertain stochastic fuzzy systems with multiple time delays," *IEEE Transactions on Systems Man and Cybernetics Part B-Cybernetics*, vol. 38, no. 1, pp. 126-140, 2008. [click]

[13] H. Zhang, J. Zhang, G. H. Yang, and Y. Luo, "Leader-based optimal coordination control for the consensus problem of multiagent differential games via fuzzy adaptive dynamic programming," *IEEE Tran. on Fuzzy Systems*, vol. 23, no. 1, pp. 152-163, 2015. [click]

[14] J. Yang, H. Su, Z. Li, D. Ao, and R. Song, "Adaptive control with a fuzzy tuner for cable-based rehabilitation robot," *Inter. J. of Control, Automation and Systems*, vol. 14, no. 3, pp. 865-875, 2016. [click]

[15] H. Zhang, D. Liu, *Fuzzy Modeling and Fuzzy Control*, Birkhäuser, Boston, 2006.

[16] S. Yang, C. Li, and T. Huang, "Exponential stabilization and synchronization for fuzzy model of memristive neural networks by periodically intermittent control," *Neural Networks*, vol. 75, pp. 162-172, 2016. [click]

[17] S. Yang, C. Li, and T. Huang, "Impulsive synchronization for TS fuzzy model of memristor-based chaotic systems with parameter mismatches," *Inter. Journal of Control, Automation and Systems*, vol. 14, no. 3, pp. 854-864, 2016. [click]

[18] S. N. Sivanandan, S. Sumathi, and S. N. Deepa, *Inductionto Fuzzy Logic Using MATLAB*, Springer, Verlag Berlin Heidelberg, 2007.

[19] O. Linda and M. Manic, "General type-2 fuzzy c-means algorithm for uncertain fuzzy clustering," *IEEE Tran. on Fuzzy Systems*, vol. 20, no. 5, pp. 883-897, 2012. [click]

[20] R. Hosseini, S. D. Qanadli, S. Barman, M. Mazinani, T. Ellis, and J. Dehmeshki, "An automatic approach for learning and tuning Gaussian interval type-2 fuzzy membership functions applied to lung CAD classification system," *IEEE Transactions on Fuzzy Systems*, vol. 20, no. 2, pp. 224-234, 2012. [click]

[21] H. F. Ho, Y. K. Wong, and A. B. Rad, "Adaptive fuzzy sliding mode control with chattering elimination for nonlinear SISO systems," *Simulation Modelling Practice and Theory*, vol. 17, pp. 1199-1210, 2009. [click]

[22] V. Nekoukar and A. Erfanian, "Adaptive fuzzy terminal sliding mode control for a class of MIMO uncertain nonlinear systems," *Fuzzy Sets and Systems*, vol. 179, pp. 34-49, 2011. [click]

[23] O. Castillo and P. Melin, "A review on the design and optimization of interval type-2 fuzzy controllers," *Applied Soft Comp.*, vol. 12, pp. 1267-1278, 2012. [click]

[24] J. L. Yao and W. K. Shi, "Development of a sliding mode controller for semi-active vehicle suspensions," *J. of Vibration and Control*, vol. 19, pp. 1152-1160, 2013.

[25] B. L. Zhang, Q. L. Han, X. M. Zhang, and X. Yu, "Sliding mode control with mixed current and delayed states for offshore steel jacket platforms," *IEEE Trans. on Con. Sys. Tech.*, vol. 22, pp. 1769-1783, 2013. [click]

[26] J. Song, S. Song, and H. Zhou, "Adaptive nonsingular fast terminal sliding mode guidance law with impact angle constrains," *Inter. J. of Control, Auto. and Systems*, vol. 14, no. 1, pp. 99-114, 2016. [click]

[27] H. Alli and O. Yakut, "Application of robust fuzzy sliding-mode controller with fuzzy moving sliding surfaces for earthquake-excited structures," *Structural Engineering and Mechanics*, vol. 26, pp. 517-544, 2007. [click]

[28] S. Mobayen and S. Javadi, "Disturbance observer and finite-time tracker design of disturbed third-order nonholonomic systems using terminal sliding mode," *Journal of Vibration and Control*, vol. 23, no. 2, 2017.

[29] G. Milad and A. Nastaran, "Fuzzy Sliding Mode Control for applying to active vehicle suspensions," *WSEAS Tran. on Systems and Cont.*, vol. 5, pp. 48-57, 2010.

[30] S. D. Nguyen and Q. H. Nguyen, "Design of active suspension controller for train cars based on sliding mode control, uncertainty observer and neuro-fuzzy system," *Journal of Vibration and Control*, vol. 23, no. 8, 2017.

[31] W. H. Chen, "Disturbance observer based control for nonlinear systems," *IEEE/ASME Transactions on Mechatronics*, vol. 9, no. 4, pp. 706-710, 2004. [click]

[32] R. Mohammad, H. Mohammad, and R. Mohammad, "An optimal and intelligent control strategy for a class of nonlinear systems: adaptive fuzzy sliding mode," *Journal of Vibration and Control*, vol. 22, no. 1, 2016.

[33] P. T. Chan, A. B. Rad, and J. Wang, "Indirect adaptive fuzzy sliding mode control: Part II: parameter projection and supervisory control," *Fuzzy Sets and Systems*, vol. 122, pp. 31-43, 2001. [click]

[34] M. A. Khanesar, O. Kaynak, S, Yin, and H. Gao, "Adaptive indirect fuzzy sliding mode controller for networked control systems subject to time-varying network-induced time delay," *IEEE Transactions on Fuzzy Systems*, vol. 23, no. 1, pp. 205-214, 2015. [click]

[35] W. H. Chen, "Nonlinear disturbance observer-enhanced Dynamic inversion control of missiles," *Journal of Guidance, Control, and Dynamics*, vol. 26, no. 1, pp. 161-166, 2003. [click]

[36] H. Li, J. Yu, C. Hilton, and H. Liu, "Adaptive sliding-mode control for nonlinear active suspension vehicle systems using T-S fuzzy approach," *IEEE Trans. on Indus. Electronics*, vol. 60, no. 8, pp. 3328-3338, 2013. [click]

[37] S. D. Nguyen and T. I. Seo, "Establishing ANFIS and the use for predicting sliding control of active railway suspension systems subjected to uncertainties and disturbances," *Inter. J. of Machine Learning and Cybernetics*, Doi: 10.1007/s13042-016-0614-z, 2016.

Sy Dzung Nguyen received the M.E. degree in Manufacturing Engineering from Ho Chi Minh City University of Technology (HCMUT) - VNU in 2001, Ph.D. degree in Applied Mechanics in 2011 from HCMUT. He was a postdoctoral fellow at Inha University, Korea, 2011-2012, at Incheon National University, Korea, 2015-2016. He is currently a Head of Division of Computational Mechatronics, Institute for Computational Science, Ton Duc Thang University, Vietnam. His research interests include artificial intelligence and its applications to nonlinear adaptive control, system identification and managing structure damage. Dr. Nguyen has been the main author of plenty of ISI papers in these fields.

Seung-Bok Choi received the B.Sc. degree in mechanical engineering from Inha University, Korea, 1979, the M.Sc. and Ph.D. degrees from the Michigan State University, U.S.A in 1986 and 1990, respectively. He is currently a dean of graduate school of Inha University and a distinguished fellow professor of mechanical engineering at Inha University. His research interests are control applications using smart materials such as electro-rheological (ER) fluids, magneto-rheological (MR) fluids, piezoelectric materials and shape memory alloys. He has published more than 450 refereed international journal papers and two books in the area of smart materials and their applications.

Tae-il Seo received the Ph.D. Degree in mechanical engineering, Ecole Centrale de Nantes, France, in 1998. From 1998 to 1999, he was a postdoctoral research fellow in Department of Mechanical Engineering in Inha University, Incheon, Korea. From 1999 to 2001, he was a research fellow in the Department of mechanical corporation Laboratory, Inha University of Korea. From 2001 to 2003, he was a researcher in Department of Precision Mold Lab, KITECH (Korea Institute of Industrial Technology), Korea. Currently, he is a Professor in Department of Mechanical Engineering in Incheon National University, Korea. Dr. Seo's current research interests include Micro End-Milling, Intelligent Manufacturing System, CAD/CAD systems, etc.